

# Region Growing Segmentation Method for Extracting Vessel Structures from Coronary Cine-angiograms

K.A.S.H. Kulathilake,  
L. Ranathunga  
Department of Information  
Technology  
University of Moratuwa  
Moratuwa, Sri Lanka  
[hemanthak@uom.lk](mailto:hemanthak@uom.lk)  
[lochandaka@uom.lk](mailto:lochandaka@uom.lk)

G.R. Constantine  
Department of Clinical Medicine  
Faculty of Medicine  
University of Colombo  
Colombo 08, Sri Lanka  
[godwinconstantine@live.com](mailto:godwinconstantine@live.com)

N.A. Abdullah  
Department of Computer System and  
Technology  
University of Malaya  
Kuala Lumpur, Malaysia  
[noraniza@um.edu.my](mailto:noraniza@um.edu.my)

**Abstract**—The coronary cine-angiogram (CCA) is an invasive medical image modality which is used to determine the luminal obstructions or stenosis in the Coronary Arteries (CA). CCA based quantitative assessment of vascular morphology is a demanding area in medical diagnosis and segmentation of blood vessels in CCAs is one of the mandatory step in this endeavor. The accurate segmentation of CAs in Angiogram is a challenging task due to various reported reasons. In order to overcome this challenge, we proposed a region growing segmentation method which implements using morphological image processing operations and flood fill method. It can extract the boundary of main CA visualized in the processed CCA completely. The result of the proposed method reveals that this proposed segmentation method possesses 90.89% accuracy to segment the CAs related to the selected Angiography views. This segmentation results can be further enhanced to determine the functional severity of the CA and this study laid the foundation to improve the Angiography based diagnosis technique.

**Keywords**—angiography, computer aided diagnosis, vessel segmentations, morphological image processing, medical diagnostic imaging

## I. INTRODUCTION

The Coronary Cine-angiogram (CCA) provides excellent visualizations of Coronary Artery (CA) vasculature and is used to detect luminal obstruction or the degree of stenosis in CAs [1][2][3]. The diagnosis based on Angiogram is subjective because the results are produced mainly through visual judgments [4]. Those visual judgments are done based on the Angiogram images taken under the limited number of views. Angiogram based quantitative assessment of vascular morphology (i.e. stenosis or CA malformations) is a demanding area in medical image processing and segmentation of blood vessels in CCAs is one of the mandatory steps in most of the published quantitative assessment procedures [1].

Segmentation subdivides an image into its constituent regions or objects [5]. It has been reported that the accurate segmentation of CAs in Angiogram is a challenging task. The major reasons for that are; poor signal to noise ratio due to the

poor X-ray penetration, overlapping vessels, superimposition of vessels with various anatomical structures such as ribs, spine or heart chambers [6] and visual degradation occurs due to the nonuniform illumination [7].

Our proposed segmentation method has been implemented through combined morphological operations and flood fill for extracting the foreground objects from direct CCAs. CAs and parts of the catheter recorded in each frame of the CCAs are considered as foreground objects. According to the proposed segmentation method, these foreground objects are extracted from the direct CCA frame through an iterative process. Those extracted foreground objects are saved into a set of new frames created corresponding to each individual frame of input CCA. These newly created frames are returned as the output of this proposed segmentation method. Moreover, this segmentation method does not depend on any kind of prior knowledge about vessel regions of CCAs.

In this study, the Left Main CA (LMA), Circumflex Artery (CXA) and Right CA (RCA) are considered as the main CAs to be extracted under the selected Angiography views. The resulting frames obtained from this method have clearly marked the boundaries of the segmented main CAs for easy identification. Moreover, these resulting frames can apply for improving Angiography such as reduction of motion artifacts, formulating some pathways to recognizing the vessels and assisting to detection and quantification of stenosis.

The rest of the paper is organized as follows: Next section explains the highlights of some related research studies. Afterwards, the proposed segmentation method is described in detail. The experimental setup of the proposed method, results and discussion on the results are reported in the fourth section. Finally, the conclusion section briefly explains the future work that can extend using the results of this proposed segmentation method.

## II. BACKGROUND OF THE STUDY

The various CA segmentation methods have been reported in the research studies published in recent past. Most of those published methods can be categorized under the criteria such

as pattern recognition approaches, model based approaches, tracking based approaches and Artificial Intelligence (AI) based approaches [2][7].

Pattern recognition techniques deal with the automatic detection or classification of objects or features. For vessel extraction, it is concerned with the automatic detection of vessel structures [2]. Multi scale methods, region growing methods, matching filter approach and mathematical morphology schemes can be considered as various approaches for pattern recognition based segmentation. Lin and Ching have published a technique for extraction Coronary Arterial tree using a frequency domain filters and matched filters [6]. Whole arterial tree was extracted from their proposed signal based image segmentation method.

Model based approaches apply explicit vessel models to extract the vasculature from CCAs. Parametric deformable models such as active contour model and snakes are one of the popular model based approached implemented on CCAs. The main disadvantage of the parametric deformable model is that it requires user interaction to initialize the model and also requires the initial parameters by the user [2]. A recent research study emphasized the application of snake model for locate the vessel boundaries of Coronary Angiograms [8]. According to the research method described in [8], the investigators have introduced a certain mechanism to overcome two problems of snake model which are lower capture range and no availability of evolution stop mechanism through dynamic gradient flow and adaptive balloon force respectively.

Tracking based approaches apply local operators on a focus known to be a vessel and track it. Vessel tracking approaches apply local operators starting from an initial point, detecting vessel centerline or boundaries by analyzing the pixels orthogonal to the tracking direction [2]. Van der Zwet, Pinto, Serruys and Reiber have invented a tracking based method to find the path lines of the CAs in Coronary Angiograms [9]. According to their investigation, the path lines were detected using two algorithms namely tracking algorithm and box algorithm. Tracking algorithm was used to find all curves in the Angiogram image which were candidates for being a path line. Box algorithm was used to provide the seed points that possibly may belong to the path line which was being searched.

AI based segmentation methods utilize knowledge to guide the segmentation process to extract the vessel structures [2]. Image acquisition technique or general blood vessel model can be used as the prior knowledge to guide the AI based segmentation process. AI based segmentation method possesses high level of accuracy but the computational complexity is much larger than the other segmentation methods.

### III. PROPOSED METHOD

The proposed method for segmentation the vessel structures from CCA is explained in this section. The Ethics Review Committee of the Faculty of Medicine, University of Colombo has granted the ethical clearance to extract the CCAs which required for validating the results of this proposed

method. As schematized in Fig. 1 the proposed method mainly consists of four major phases namely, pre-processing, generating the mask image, foreground extraction and vessel boundary detection. Following sections briefly explain the main steps of each of aforementioned segmentation phases of the proposed method.

#### A. Pre-processing Phase

It was published that the CCA frames consist of salt and pepper noise and nonuniform illumination [7]. As a result of that, the visual quality of the recorded CCA is degraded. Therefore, the objective of the pre-processing phase is to apply possible image enhancement techniques to obtain the required visual quality of the vessel structures of the CCAs by reducing noise and nonuniform illumination. A median filter with kernel size  $3 \times 3$  was applied to the CCA frames as a noise removal technique. Afterwards a homomorphic filter was applied to remove the illumination component of the CCA frames. The implemented pre-processing technique is described in our other publication descriptively [10]. The processed frames are normalized to obtain the best quality contrast among the vessel structures. Equation (1) explains the normalization operation applied in this pre-processing phase.

$$I_1(x, y) = \begin{cases} M_d + \sqrt{\frac{V_d(I_0(x, y) - M)^2}{V}} & \text{if } (I_0(x, y) > M) \\ M_d + \sqrt{\frac{V_d(I_0(x, y) - M)^2}{V}} & \text{otherwise} \end{cases} \quad (1)$$

Where,  $M$  and  $V$  denote the estimated mean and variance of input frame and  $M_d$  and  $V_d$  are desired mean and variance values respectively.  $I_1(x, y)$  is the output image and  $I_0(x, y)$

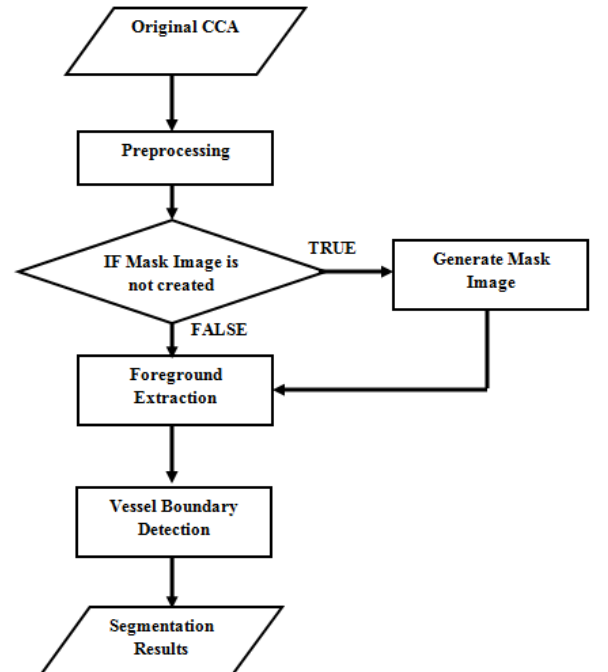


Fig. 1. The flow chart of the proposed method.

denotes the uniformly illuminated frame where  $x$  and  $y$  represents the pixel position of both input and output frames. According to the experimental results  $M_d$  was set as  $M/2$  and  $V_d$  was set as  $(V \times 4)$  to obtain better results. Furthermore, the values for both  $M_d$ ,  $V_d$  parameters of normalization can be changed in different experimental setups. Fig. 2 depicts an original CCA frame and the respective pre-processed CCA frame for further clarification.

### B. Generating Mask Image

During this proposed segmentation method, there is a possibility to segmenting nonvessel regions as expected vessel tree components. These incorrectly segmented nonvessel regions are considered as noise regions and it is required to identify the foreground and background regions of each CCA frame separately, to reduce the formation of such noise regions. The vessel region visualized in the CCA frame is considered as the foreground and the mask image created in this phase is directly used to extract the foreground regions during the next implementation phase of the proposed segmentation method.

Mask image creation phase consists of two major steps namely; detecting the total foreground area and enhancement. The initial model of the mask is formed in detection of total foreground area and is done iteratively using the pre-processed CCA frames. Within the iteration, three operations are employed to two consecutive frames of the CCA. As the first operation, it computes the frame difference between two consecutive frames of the input CCA to be processed. This frame difference results depicts the common area where the foreground objects (vessels in this application) are moving within the CCA frame. As the second operation, threshold is applied to the frame difference results to remove the noise regions. Afterwards, this thresholded frame difference result image is added to another matrix to form the initial mask image. These three operations are employed in remaining iterations to obtain the initial mask image. The initial mask image contains the total region where the foreground objects (vessels in this application) are moving within the all frames of processed CCA. The sample initial mask image is depicted in Fig. 3(a).

Within the enhancement step, the initial mask image created in the previous step of this phase is further processed to improve the visual clarity of its background and foreground regions. In order to achieve that, the binary version of the initial mask image is created. In this operation, all white pixels in the initial mask image are remained as it is and other pixels are updated as black (Fig. 3(b)). White pixels of the binary mask image represent the common foreground area (vessels)



Fig. 2. Pre-processing step; (a) frame extraction from direct CCA, (b) corresponding pre-processed frame of (a).

and black pixels model the common background area of the processed CCA. The tiny white blobs in binary mask image (area  $< 10$ ) are removed as the second operation of this step and it emphasized the foreground region of the mask image greatly (Fig. 3(c)). Afterwards, the morphological dilation operation was applied three times to mask image to merge concave areas within the foreground region and expand the foreground region (Fig. 3(d)).

### C. Foreground Extraction

Vessel region isolation and extraction are done in the foreground extraction phase. A preprocessed CCA and mask image created in the previous phase are input to this foreground extraction phase and it iteratively processes the individual frames to extract the vessel regions as the foreground. A set of frames visualizes the extracted vessel regions are produced as the output of the foreground extraction phase. In order to obtain the expected output, a series of image processing steps have been applied to each individual frame of input CCA and those operations are explained in detail in the following sections.

As the initial step of foreground extraction phase, a threshold function is applied to the input preprocessed frames to further enhance the contrast of the vessel regions. In order to achieve that, a minimum intensity value (0 in this operation) is set to the potential vessel regions of the currently process frame by this threshold function. The threshold function used in this step is shown in following (2);

$$I_2(x, y) = \begin{cases} I_1(x, y) & \text{if } I_1(x, y) > T \\ 0 & \text{otherwise} \end{cases} \quad (2)$$

Where,  $I_1(x, y)$  is the preprocessed frame and  $I_2(x, y)$  is the resulting frame.  $x$  and  $y$  denote the pixel position of both input

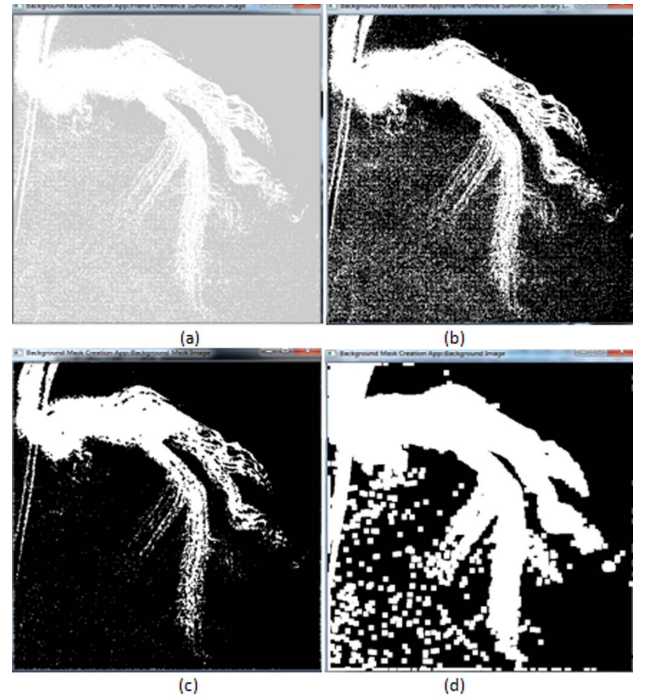


Fig. 3. Mask image creation; (a) initial mask image, (b) binary version of initial mask image, (c) tiny blobs removed mask image, (d) dilated mask image.



and output frames.  $T$  denotes the threshold value and is vary depending on the special aspects of input CCA. The effect of this threshold function is depicted in Fig. 4.

Morphological erosion operation was applied to the  $I_2(x, y)$  frame followed by the threshold function. It is iterated three times on the  $I_2(x, y)$  frame and the result frame is denoted as  $I_3(x, y)$ . As a result of erosion operation, the darker regions in the frame are expanded. As a result of this expansion, some expanded background regions are also merged with the vessel regions visualized in  $I_2(x, y)$ . Fig. 5(a) depicts the resulting frame ( $I_3(x, y)$ ) obtained after the erosion operation. Experimental results have revealed that these additionally merged regions lead to form the noisy segmented regions and are affected to the accuracy of proposed segmentation method. In order to get rid from this noise region segmentation problem, a background subtraction step is applied to  $I_3(x, y)$  frame by using the mask image created in the background mask creation phase.

As the third step, the foreground regions of the  $I_3(x, y)$  frame is extracted by subtracting the background regions and it is done using the function given in (3);

$$I_4(x, y) = \begin{cases} I_3(x, y) & \text{if } M(x, y) = 255 \\ K, & \text{otherwise} \end{cases} \quad (3)$$

Where  $I_4(x, y)$  is the reconstructed background subtracted frame and  $I_3(x, y)$  is the eroded frame obtained in the previous step.  $M(x, y)$  is the background mask image and  $K$  is a specific gray value assigned to the subtracted background regions of the resulting frame  $I_4(x, y)$ .  $x$  and  $y$  denote the pixel position of both input and output frames. Resulting frame obtained in this step is depicted in Fig. 5(b).

After the background subtraction step, the flood fill operation is applied to the  $I_4(x, y)$  frame to extract the vessel regions from the marked foreground. Seed point is selected manually from the catheter engaged point in  $I_4(x, y)$  frame. Therefore, the gray value of seed point is set as '0' for all cases. Based on the empirical results, the lower bound intensity for the flood fill operation was selected as '0' and upper bound intensity was selected as 8. Flood filled frame is denoted as  $I_5(x, y)$  and the flood filled region is filled in white color. It is depicted in Fig. 5(c).

Final step of the foreground extraction phase is creating a new frame of vessel regions using the flood filled frame produced in the previous step ( $I_5(x, y)$ ). The result frame

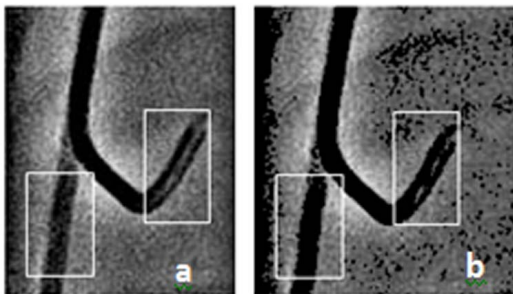


Fig. 4. Threshold function ( $T=63$ ); (a) section of input frame, (b) enhanced frame; marked areas represent the improved regions.

created in this step is denoted as  $I_6(x, y)$  and is generated using the function given in (4).

$$I_6(x, y) = \begin{cases} I_1(x, y) & \text{if } I_5(x, y) = 255 \\ K, & \text{otherwise} \end{cases} \quad (4)$$

Where,  $I_6(x, y)$  is the newly created result frame which contains the foreground of the input CCA frame.  $I_5(x, y)$  is the flood filled frame and  $I_1(x, y)$  is the preprocessed frame.  $K$  is a specific gray value assigned to background of the  $I_6(x, y)$  frame.  $x$  and  $y$  denote the pixel position of both input and output frames. Resulting frame  $I_6(x, y)$  obtained in this step is depicted in Fig. 5(d).

#### D. Vessel Boundary Detection

The final phase of the proposed segmentation method is detection of vessel boundaries through contour detection. In order to achieve that, a binary image is created using the output frame obtained in the foreground extraction phase (It is done using  $I_6(x, y)$ ). This newly created image is denoted as  $I_7(x, y)$  and it is depicted in Fig. 6(a). Contour detection is done using this  $I_7(x, y)$  image and detected contours are marked in  $I_1(x, y)$  frame for visualization (Fig. 6(b)).

$$\alpha + \beta = \chi. \quad (1) \quad (1)$$

#### IV. RESULTS AND DISCUSSION

The direct CCAs produced by Philips Medical System are used for the experiments and those were recorded in frame rate of 15fps with  $512 \times 512$  resolution. In order to validate this proposed segmentation method, we have run the developed algorithm of the proposed method using the data set of fifteen randomly selected angiogram cases. The information about the

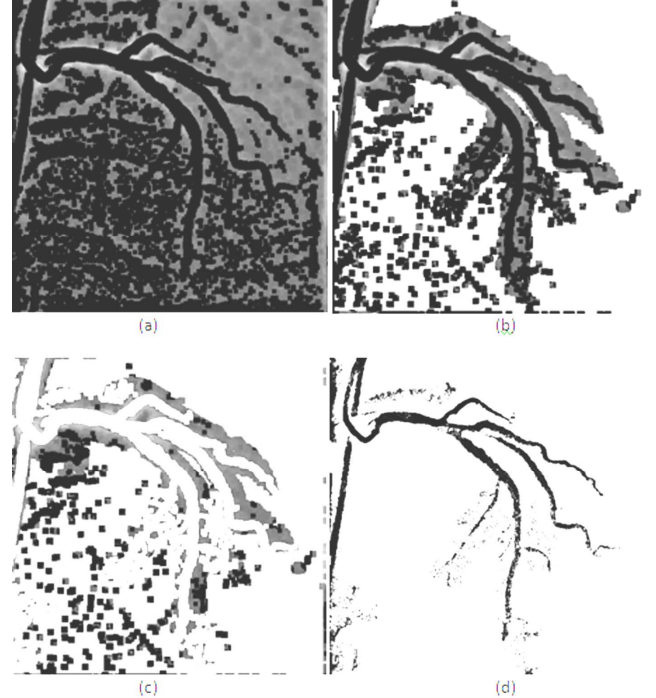


Fig. 5. Results of foreground extraction step; (a) Eroded frame, (b) background subtracted frame, (c) flood filled frame, (d) foreground extracted frame.

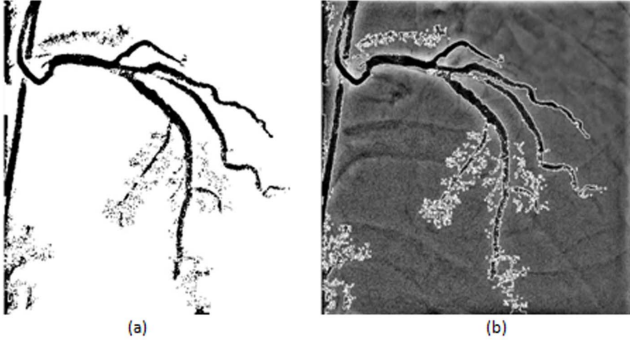


Fig. 6. Detection of vessel boundaries, (a) binary image created using  $I_0(x, y)$ . (b) detected vessel boundaries.

selected dataset for the validation is listed in Table I. According to the Table I, each case consists of three CCA which recorded under the three standard Angiography views namely; RCA Left Anterior Oblique Cranial (RAO-CRA), Anterior Posterior Caudal (AP-CODL) and Anterior Posterior Cranial (AP-CRNL). We have selected CCAs under aforementioned views because those views provide the best visualizations for RCA, CXA and LMA respectively. Further, Table I enlists the total number of frames for each CCA which are used to validate the proposed segmentation method. Hence, we analyzed 1152 total frames under the 45 total CCAs to validate the accuracy of this proposed method. The seed point for the flood fill operation was set manually for each execution.

The percentage of successfully segmented frames out of the total number of frames of each CCA is used as the measurement to determine the accuracy of the proposed segmentation method and is denoted as the True Positive Percentage (TP%). Table I lists the TP% for each CCA case as the validation results. Further, Table II lists the summary results according to the selected angiogram views and it reveals that this proposed segmentation method possesses 90.89% accuracy to segment the CAs related to the selected Angiography views. In addition to that, to visually compare the results, a set of visual frames of a selected test case is depicted in Fig. 7 and the respective segmentation results obtained for the same test case is depicted in Fig. 8. Further, Fig. 8 clearly depicts the extracted complete vessel tree in each frame of the selected test case. Moreover, the proposed method is fully eliminated the background anatomical structures such as ribs, heart and lungs which recorded in the original CCAs. Due to this, it is easy to detect the contours of the vessel regions.

This proposed segmentation method is implemented based on a set of basic morphological image processing operations. Therefore, it is computationally efficient and methodically simple when comparing with AI based vessel segmentation methods. Further, this proposed segmentation method does not depend on any kind of prior information. Therefore, this method is a straight forward when comparing with the model based segmentation methods.

Further, the empirical results have revealed that this proposed segmentation method failed to extract major vessels

under the poor intensity conditions. It has been identified following constraints of this proposed segmentation method to obtain the successful results: (1) visualizing clear contrast agent flow within a lower intensity depth of input CCA, (2)

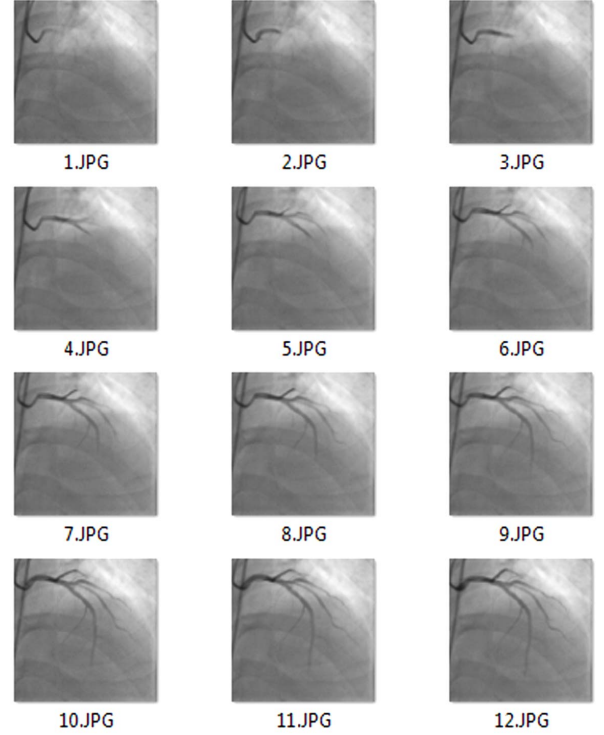


Fig. 7. Original frames of a selected test case.

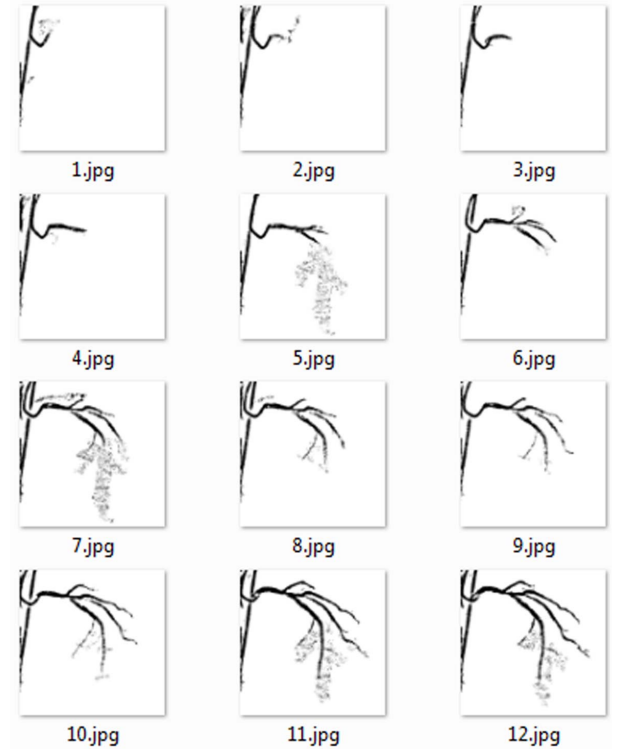


Fig. 8. Segmentation results.

TABLE I. DATA SET USED FOR VALIDATION AND TRUE POSITIVE (TP) MATCHING PERCENTAGE

CASE No.	RAO-CRA for RCA		AP-CODL for CXA		AP-CRNL for LMA	
	No. of Frames	TP %	No. of Frames	TP%	No. of Frames	TP%
1	20	100.00	14	71.43	24	87.50
2	24	87.50	22	100.00	45	88.89
3	21	90.48	27	88.89	13	92.31
4	20	85.00	17	94.12	20	100.00
5	16	87.50	23	100.00	19	89.47
6	18	100.00	24	100.00	19	89.47
7	31	87.10	37	97.30	37	100.00
8	34	79.41	37	91.89	31	90.32
9	30	90.00	35	91.43	31	87.10
10	29	100.00	37	83.78	21	85.71
11	22	100.00	25	80.00	19	84.21
12	41	97.56	33	84.85	25	100.00
13	31	90.32	24	91.67	19	100.00
14	25	92.00	24	87.50	25	88.00
15	13	76.92	25	84.00	25	88.00

TABLE II. SUMMARY RESULTS ACCORDING TO THE ANGIOGRAPHY VIEW

	RAO-CRA for RCA	AP-CODL for CXA	AP-CRNL for LMA
Total Frames	375	404	373
Total TP frames	342	364	341
Total TP%	91.20	90.10	91.42

projecting nonoverlapped vessels to minimize the ambiguities of the structure, and (3) recording noise free background during the Angiography procedure.

## V. CONCLUSION

In this study, we proposed a region growing segmentation method to extract the main vessel regions recorded in the CCA. The proposed method has been implemented combining morphological image processing methods and region growing based segmentation method called flood fill. The result of the proposed method reveals that this proposed segmentation method possesses 90.89% accuracy to segment the CAs related to the selected Angiography views. Further, visual frames consist of clearly segmented main vessel regions of the CAs under the selected Angiography views. Moreover, the background mask applied in this proposed method minimizes the segmenting nonvessel regions of the CCA frame as the expected vessel region. It assists to extract the vessel regions correctly during the segmentation process.

As the future work, we expect to find the adaptive threshold mechanism for vessel structure extraction steps of this proposed method to minimize the noisy segmentation. Further, the segmentation results of this method will provide the foundation to determine the functional severity of the CA based on the flow rate calculation of the segmented vessels.

## ACKNOWLEDGEMENT

This investigation received financial support from the National Science Foundation, Sri Lanka under Grant No. NSF/SCH/2013/06. The authors thank the staff of the Cardiology Unit of the National Hospital Sri Lanka.

## REFERENCES

- [1] G. C. Kagadis, P. Spyridonos, D. Karnabatidis, A. Diamantopoulos, E. Athanasiadis, A. Daskalakis, K. Katsanos, D. Cavouras, D. Mihailidis, D. Siablis, and G. C. Nikiforidis, "Computerized analysis of digital subtraction angiography: A tool for quantitative in-vivo vascular imaging," *J. Digital Imaging*, vol. 21, no. 4, pp. 433–445, Dec. 2008.
- [2] C. Kirbas and F. Quek, "A review of vessel extraction techniques and algorithms," *ACM Computing Surveys*, vol. 36, no. 2, pp. 81–121, Jun. 2004.
- [3] G. S. Wagner, O. Pahlm, and N. Kjell C., "Chapter 4 - Coronary Angiography," in *Multimodal Cardiovascular Imaging: Principles and Clinical Applications*, 1st ed., McGraw-Hill Medical, 2011, pp. 71–80.
- [4] J. T. Wong, H. Le, W. M. Suh, D. A. Chalyan, T. Mehraien, M. J. Kern, G. S. Kassab, and S. Molloy, "Quantification of fractional flow reserve based on angiographic image data," *Int. J. Cardiovascular Imaging*, vol. 28, no. 1, pp. 13–22, Jan. 2012.
- [5] R. C. Gonzalez and R. E. Woods, "Image segmentation," in *Digital Image Processing*, 3rd ed., Addison-Wesley Pub (Sd), 1992, pp. 689–794.
- [6] C.Y. Lin and Y.T. Ching, "Extraction of coronary arterial tree using cine X-ray angiograms," *Biomedical Eng. Applicat. Basis Commun.*, vol. 17, no. 03, pp. 111–120, Jun. 2005.
- [7] M. T. Dehkordi, S. Sadri, and A. Doosthoseini, "A review of coronary vessel segmentation algorithms," *J. Medical Signals Sensors*, vol. 1, no. 1, pp. 49–54, Jan. 2011.
- [8] S. Nirmala Devi and N. Kumaravel, "Comparison of active contour models for image segmentation in X-ray coronary angiogram images," *J. Medical Eng. Technol.*, vol. 32, no. 5, pp. 408–418, Jan. 2008.
- [9] P. M. J. van der Zwet, I. M. F. Pinto, P. W. Serruys, and J. H. C. Reiber, "A new approach for the automated definition of path lines in digitized coronary angiograms," *Int. J. Cardiac Imaging*, vol. 5, no. 2, pp. 75–83, Jun. 1990.
- [10] K. A. S. H. Kulathilake, L. Ranthunga, G. Constantine, and N. A. Abdullah, "Hierarchical region based template matching technique for global motion reduction of coronary cineangiograms," *Int. J. Comput. Theory Eng.*, vol. 7, no. 2, pp. 156–161, Apr. 2015.